Journal of
Ship&Ocean
Technology
©JUNE 2002

SOTECH Vol. 6, No. 2, pp. 1~11, 2002

Vibration Power Flow Analysis of Submarine-shaped Structures using Developed Software

Seong-Hoon Seo[1] and Suk-Yoon Hong[1]

[1]Department of Naval Architecture and Ocean Engineering, Seoul National University, San 56-1, Shillim-dong, Kwanak-gu, Seoul 151-742, Korea; E-mail: syhong@gong.snu.ac.kr

Abstract

For the analysis of vibrational energy density and intensity of partitioned complex system structures in medium-to-high frequency ranges, A software based on the Power Flow Analysis(PFA) has been developed for the plate elements. The flexural, longitudinal and shear waves in plates are formulated and the joint element equations for multi-coupled plates are fully developed. Also, the wave transmission approach has been introduced to cover the energy transmission and reflection at the joint plate elements. To confirm the validity of the developed PFA software, the submarine-shaped complex structures are used for the analysis of vibration intensity and energy density.

Keywords: power flow analysis, power flow finite element method, vibration analysis, medium-to high frequency

1 Introduction

In the structures vibrational energy flows along the frame and causes structure-borne noise in places far from its source. For example, the vibrational energy generated by the marine propulsion power system is transmitted to various parts of the hull through structural frameworks like mounts, decks, partitions and so on. An amount of the transmitted energy is radiated as unwanted sound in inhabited space to annoy the crews and the passengers and also in the water. The most widely used method for the suppression of the structure-borne noise, is to increase the attenuation of structure-borne noise through damping treatments on the paths along which the energy travels. Thus, for vibration analysis of large structures like the ships, automobiles and aircraft, it is absolutely necessary to understand energy density distributions and energy flow paths of the structures.

The Finite Element Method(Zienkiewicz and Tayler 1989) for predicting structure-borne noise is effectively applied at low frequencies. At high frequency ranges, however, the FEM is ineffective due to the requirement that the mesh size be small enough which makes model generation, turn-around time, and computation cost high. At high frequency ranges, Statistical Energy Analysis(Lyon and DeJong 1995) is used to predict global behavior of built-up structures. SEA, however, has several weaknesses as it does not provide information about the variation of the responses within the subsystems nor can it be applied at medium frequency ranges where the modal density of structures is not high enough.

Power Flow Analysis(PFA), analogous to the steady-state heat flow analysis has been suggested as one of the promising method to solve the above-mentioned problems seen in medium-to-high frequency ranges(Belov et al 1977). Since energy governing equations based on PFA are derived using a differential volume approach, it can predict the spatial variation of energy density or power flow in a subsystem and the effects of local damping treatments or local power inputs in a straightforward manner. In the case of analyzing large complex structures with PFA, so many boundary conditions and arbitrary shapes of elements make it difficult to solve energy governing equations analytically. The Power Flow Finite Element Method(PFFEM) which applies the finite element method to PFA, could implement PFA method effectively for the built-up structures(Nefske and Sung 1989). The PFFEM can develop the FEM model used in low frequency analysis, and can predict the vibrational response at even much higher frequencies than that of the conventional FEM since time- and space-averaged energetics is used. In our previous work, the PFFEM was performed to analyze flexural, torsional and longitudinal waves considering coupled effects for the 1D element, beam. For the 2D element, plate, it was accomplished just as well in analyzing only flexural wave of a simple plate or coplanar plate structures.

In this work PFFEM software for the plate elements is developed and applied to several models for the extension of PFFEM analysis of vibration to partitioned complex structures similar to the actual state at medium-to-high frequency ranges. A PFFEM formulation is developed to cover the flexural, longitudinal and shear waves in plates, and joint element equations for multi-coupled plates are developed with the wave transmission approach introduced to express the energy transmission and reflection at the joint. To confirm the validity of the developed PFFEM software, submarine-shaped complex structures are analyzed with this, and the distributed energy density and intensity are successfully obtained.

2 Power flow finite element method

Bouthier and Bernhard(1992) and Park et al(2001) respectively derived the second-order energy governing differential equations for the propagation of flexural waves and in-plane waves in a steady-state as

$$-\frac{c_{gm}^2}{\eta\omega}\nabla^2\langle e\rangle_m + \eta\omega\langle e\rangle_m = \Pi_m \tag{1}$$

where ω is the angular frequency, η is the structural loss factor in the plate, subscript m means one of flexural, longitudinal and shear waves, $\langle e\rangle_m$ is time- and space(half wavelength)-averaged energy density of the m-type waves, c_{gm} is the group velocity of the m-type waves and Π is input power to the structure. The time- and space(half wavelength)-averaged farfield smoothed power flows of flexural waves and in-plane waves in a thin plate is given by

$$\langle I\rangle_m = -\frac{c_{gm}^2}{\eta\omega}\nabla\langle e\rangle_m \tag{2}$$

To implement (1) numerically with finite element method, the weak form variational statement by using the gradient and divergence theorems, can be written as

$$\int_D \{\frac{c_{gm}^2}{\eta\omega}\nabla\langle e\rangle_m \cdot \nabla\nu + \eta\omega\langle e\rangle_m\nu\}dD = \int_D \Pi_m\nu dD + \int_\Gamma \nu(-n)\cdot\langle I\rangle_m d\Gamma \tag{3}$$

where n is a unit vector normal to the element boundary D, and ν is the test fuction. For a Galerkin weighted residual scheme, the approximations are made as

$$\langle e \rangle_m = \sum_j e_{mj} \phi_j \tag{4}$$

$$\nu = \sum_i \phi_i \tag{5}$$

Substituting (4) and (5) into (3) yields the following matrix equation

$$\left[K_m^{(e)}\right] \left\{e_m^{(e)}\right\} = \left\{F_m^{(e)}\right\} + \left\{Q_m^{(e)}\right\} \tag{6}$$

where

$$K_{mij}^{(e)} = \int_D \{\frac{c_{gm}^2}{\eta\omega} \nabla\phi_i \cdot \nabla\phi_j + \eta\omega\phi_i\phi_j\} dD \tag{7}$$

$$F_{mi}^{(e)} = \int_D \Pi_m \phi_i dD \tag{8}$$

$$Q_{mi}^{(e)} = \int_\Gamma \frac{c_{gm}^2}{\eta\omega} \phi_i(-n) \cdot \nabla\langle e \rangle_m d\Gamma \tag{9}$$

Here, $K_{mij}^{(e)}$ is a term in the coefficient matrix which contains both stiffness- and mass-matrix terms, $F_{mi}^{(e)}$ is the input power and $Q_{mi}^{(e)}$ is power flow of which the positive direction is defined as a vector into its element. The global matrix equations for the flexural, longitudinal and shear waves of the plates can be represented by assembling the element matrix (6) as

$$\begin{bmatrix} K_f & & \\ & K_l & \\ & & K_s \end{bmatrix} \begin{Bmatrix} e_f \\ e_l \\ e_s \end{Bmatrix} = \begin{Bmatrix} F_f \\ F_l \\ F_s \end{Bmatrix} + \begin{Bmatrix} Q_f \\ Q_l \\ Q_s \end{Bmatrix} \tag{10}$$

where subscripts f, l and s mean flexural, longitudinal and shear wave, respectively. For the discontinuity of energy density at a joint, it is necessary to insert joint elements at the joint to connect the coupled structural elements. The joint element matrix equations for multi-coupled plates are

$$\begin{Bmatrix} Q_f \\ Q_l \\ Q_s \end{Bmatrix} = [P - I][C][P + I]^{-1} \begin{Bmatrix} e_f \\ e_l \\ e_s \end{Bmatrix} \tag{11}$$

where the power coefficient matrix, $[P]$ is composed of the m_2-type wave power transmission coefficient, $\tau_{m_1 m_2 ij}$ and reflection coefficient, $\gamma_{m_1 m_2 ij}$, in plate j due to the incident m_1-type

wave in plate i, and is represented as

$$[P] = \begin{bmatrix} \gamma_{ff11} & \tau_{ff21} & \cdots & \tau_{ffn1} & \gamma_{lf11} & \tau_{lf21} & \cdots & \tau_{lfn1} & \gamma_{sf11} & \tau_{sf21} & \cdots & \tau_{sfn1} \\ \tau_{ff12} & \gamma_{ff22} & \cdots & \tau_{ffn2} & \tau_{lf12} & \gamma_{lf22} & \cdots & \tau_{lfn2} & \tau_{sf12} & \gamma_{sf22} & \cdots & \tau_{sfn2} \\ \cdots & \cdots & \ddots & \cdots & \cdots & \cdots & \ddots & \cdots & \cdots & \cdots & \ddots & \cdots \\ \tau_{ff1n} & \tau_{ff2n} & \cdots & \gamma_{ffnn} & \tau_{lf1n} & \tau_{lf2n} & \cdots & \gamma_{lfnn} & \tau_{sf1n} & \tau_{sf2n} & \cdots & \gamma_{sfnn} \\ \gamma_{fl11} & \tau_{fl21} & \cdots & \tau_{fln1} & \gamma_{ll11} & \tau_{ll21} & \cdots & \tau_{lln1} & \gamma_{sl11} & \tau_{sl21} & \cdots & \tau_{sln1} \\ \tau_{fl12} & \gamma_{ff22} & \cdots & \tau_{fln2} & \tau_{ll12} & \gamma_{ll22} & \cdots & \tau_{lln2} & \tau_{sl12} & \gamma_{sl22} & \cdots & \tau_{sln2} \\ \cdots & \cdots & \ddots & \cdots & \cdots & \cdots & \ddots & \cdots & \cdots & \cdots & \ddots & \cdots \\ \tau_{fl1n} & \tau_{ff2n} & \cdots & \gamma_{flnn} & \tau_{ll1n} & \tau_{ll2n} & \cdots & \gamma_{llnn} & \tau_{sl1n} & \tau_{sl2n} & \cdots & \gamma_{slnn} \\ \gamma_{fs11} & \tau_{ff21} & \cdots & \tau_{fsn1} & \gamma_{ls11} & \tau_{ls21} & \cdots & \tau_{lsn1} & \gamma_{ss11} & \tau_{ss21} & \cdots & \tau_{ssn1} \\ \tau_{fs12} & \gamma_{ff22} & \cdots & \tau_{fsn2} & \tau_{ls12} & \gamma_{ls22} & \cdots & \tau_{lsn2} & \tau_{ss12} & \gamma_{ss22} & \cdots & \tau_{ssn2} \\ \cdots & \cdots & \ddots & \cdots & \cdots & \cdots & \ddots & \cdots & \cdots & \cdots & \ddots & \cdots \\ \tau_{fs1n} & \tau_{ff2n} & \cdots & \gamma_{fsnn} & \tau_{ls1n} & \tau_{ls2n} & \cdots & \gamma_{lsnn} & \tau_{ss1n} & \tau_{ss2n} & \cdots & \gamma_{ssnn} \end{bmatrix} \tag{12}$$

The group velocity matrix $[C]$ is a diagonal matrix composed of the group velocity of waves in each coupled plate. In (11), the joint element matrix $[J]$, which implies the relationships of the energy flow and the energy density at a joint of multi-coupled plates, is written as

$$[J] = [P - I][C][P + I]^{-1} \tag{13}$$

When (11) is substituted into (10), the final matrix equations of PFFEM for complex plate structures is obtained as

$$[K - J]\begin{Bmatrix} e_f \\ e_l \\ e_s \end{Bmatrix} = \begin{Bmatrix} F_f \\ F_l \\ F_s \end{Bmatrix} \tag{14}$$

3 Applications of power flow finite element

In this section, the implementation steps of the developed software for the power flow finite element method are outlined, and the analysis results of submarine-shaped structure models are discussed. The developed software is composed of three entries(pre-, main, post-processor) as presented in Table 1. In the pre-processor, first the geometry and material property data of the power flow finite element model are generated by reading input-files or importing from a general purpose pre-processor. Next, the joint element data for covering discontinuous energy density at joints, are generated by analyzing preliminarily created raw data. In the main process, stiffness elemental matrices(EK) of plate structural element and power elemental matrices(EF) are generated using general finite element techniques such as coordinate transformation, element mapping, numerical integration, etc. Also joint elemental matrices(EJ2, EJ3, EJ4) are respectively calcuated for 2, 3, and 4 plate-coupled joint structures. Then global matrices(GK, GF, GJ) are obtained by assembling these elemental matrices. In the post-processor, the energy density of each node with 3 DOFs is obtained by solving linear equtions for final PFFEM formulation. Then intensity of each node is calculated using energy density result.

One of the main objectives of this work is to demonstrate the applicability of the developed software in analyzing partitioned complex structures. For this purpose, an actual half-scale USS

submarine is selected as an object structure. The main dimensions of the analysis model are: LOA $21m$; PMB diameter $3.2m$. A uniform thickness is considered for all plate elements of the submarine. The submarine is depicted in Figure 1 modeled with the pre-processor of the software. For modeling, 1497 external nodes and 1299 structural elements are used, and the pre-processor of the software generates 2027 multiple nodes and 1540 joint elements at the joints of the model. There are a total 3524 internal nodes, and 10572 nodes for power flow finite element analysis to consider flexural, longitudinal and shear waves. Excitation with $100N$ is applied in the center of the compartment where the engine is installed. The 2kHz 1/3 octave frequency band for excitation and 0.01 internal loss factor for all plate elements are selected. The analysis results for the energy density levels of flexural waves are shown in Figure 2. As expected, energy density level is highest at the exciting position, and decays everywhere and then is lowest at the bows farthest from the source position. And also discontinuous energy density is identified at the joints. Figure 3 shows the intensity fields of flexural waves predicted by the software. It can be observed that intensity vectors spread up and down at the stern, which is due to higher power transferred to the lateral outer shell adjacent to inner plates from the floor driven by the engine source. The length of the model is much greater than its breadth by 0.15 slenderness so the variation of energy density occurs in its length direction and the attenuation at the joints of partition is bigger than that of the deck on the outer shell as expected.

For next analysis, the effect of frequency and damping loss factor is examined. Figure 4 and 5 show energy density levels for center frequencies for excitation are 2kHz and 200Hz respectively. As expected the higher frequency is, the more energy density decays. Figure 6 shows energy density levels when damping loss factor increases to 0.05 on only engine room parts and frequency is 2kHz. Energy density decays a little more in the damping-treated parts, compared with Figure 4.

4 Conclusion

The power flow finite element formulations are derived to express 3 kinds of waves in plates generated by wave mode conversion at the joint of complex structures, and joint element equations for multi-coupled plates are fully developed. Also, to validate the developed software, submarine-shaped structures are modeled and energy density and intensity are predicted using a developed pre-, main, and post-processors. The analysis results show that the software can be used as a tool of next generation for the vibration analysis and prediction in shipbuilding, aerospace and automobile industries.

References

LYON, R.H. AND DEJONG, R.G. 1995 Theory and Application of Statistical Energy Analaysis. Second Edition, Butterworth-Heinemann

BELOV, V.D., RYBAK, S.A. AND TARTAKOVSKII, B.D. 1977 Propagation of Vibrational Energy in absorbing Structures. Journal of Soviet Physics Acoustics, **23**, 2, pp. 115-119

BOUTHIER, O.M. AND BERNHARD. R.J. 1992 Models of Space-Averaged Energetics of Plates. AIAA J., **30**, 3, pp. 616-623

CHO, P.E. 1993 Energy Flow Analysis of Coupled Structures. ph. D. Dissertation Purdue University

NEFSKE, D.J. AND SUNG, S.H. 1989 Power Flow Finite Element Analysis of Dynamic Systems : Basic Theory and Application to Beams. Journal of Vibration, Acousitcs, Stress, and Reliability in Disign, **111**, pp. 94-100

PARK, D.H., HONG, S.Y., KIL, H.G. AND JEON, J.J. 2001 Power Flow Models and Analysis of In-Plane Waves in Finite Coupled Thin Plates. Jounral of Sound and Vibration, **244**, 4, pp. 651-668

WOHLEVER, J.C. AND BERNHARD, R.J. 1992 Mechanical Energy Flow Models of Rods and Beams. Journal of Sound and Vibration, **153**, 1, pp. 1-19

ZIENKIEWICZ, O.C. AND TAYLER, R.L. 1989 The Finite Element Method. Forth Edition, McCraw Hill, England

Table 1: Flowchart of power flow finite element programs

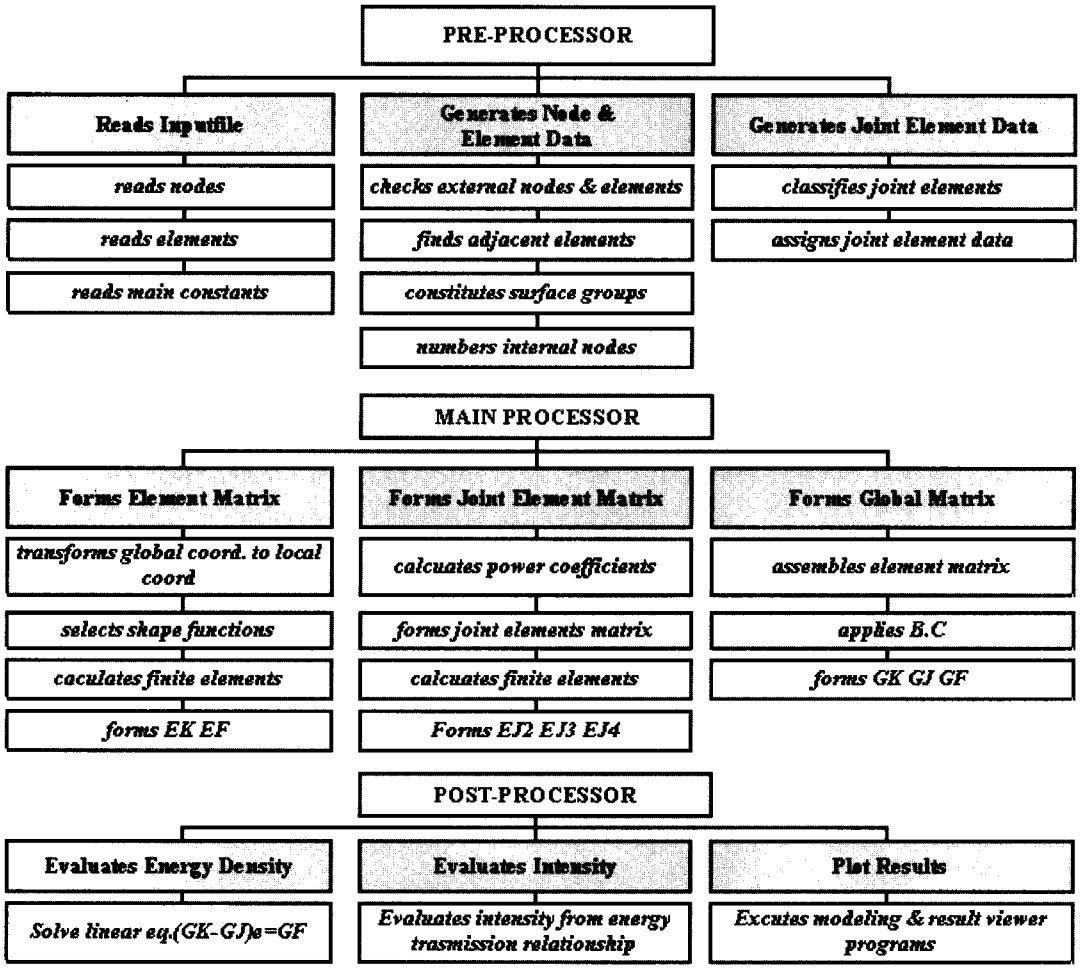

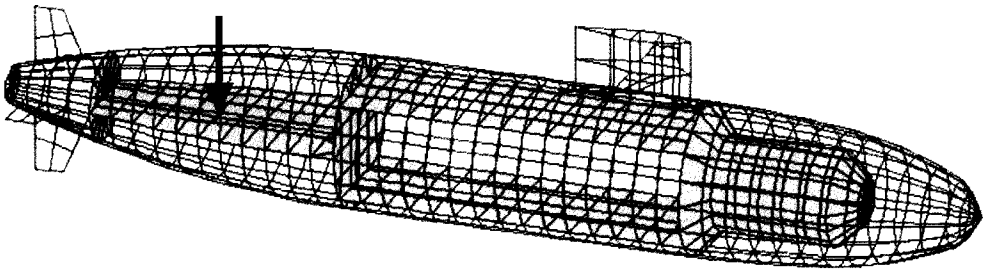

Figure 1: Modeling of submarine-shaped structures

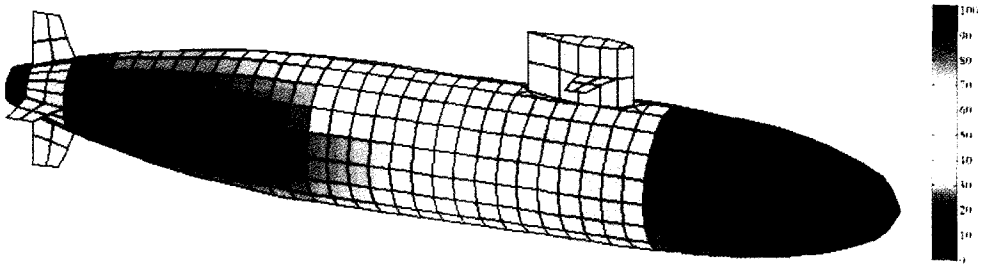

(a) Exterior

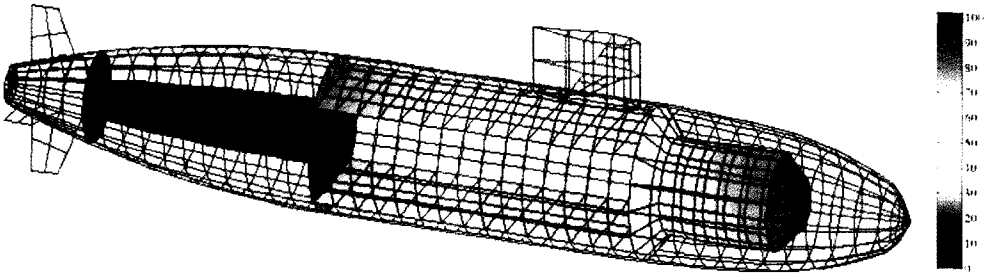

(b) Interior

Figure 2: Flexural energy density fields when f=5kHz and η=0.01

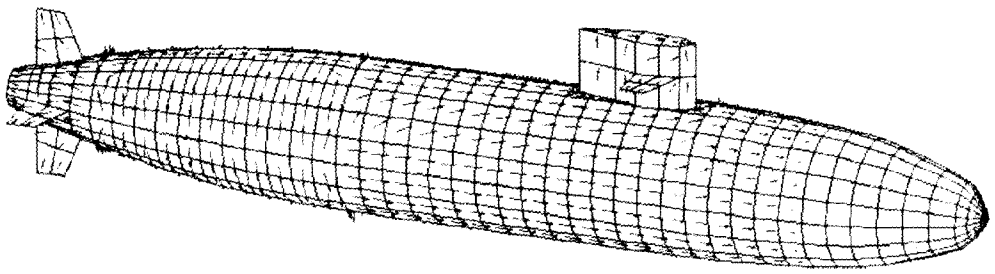

(a) Exterior

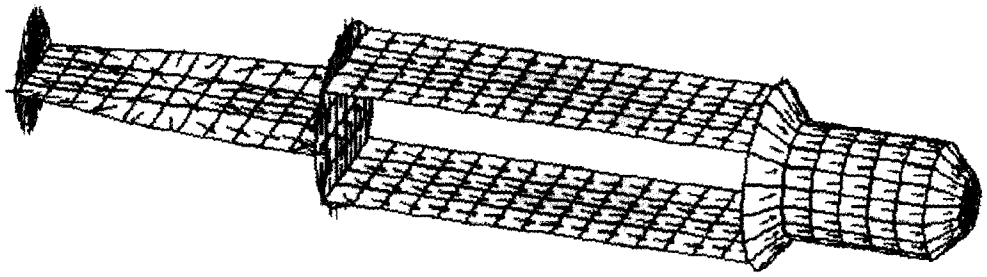

(b) Interior

Figure 3: Flexural intensity density fields when f=5kHz and η=0.01

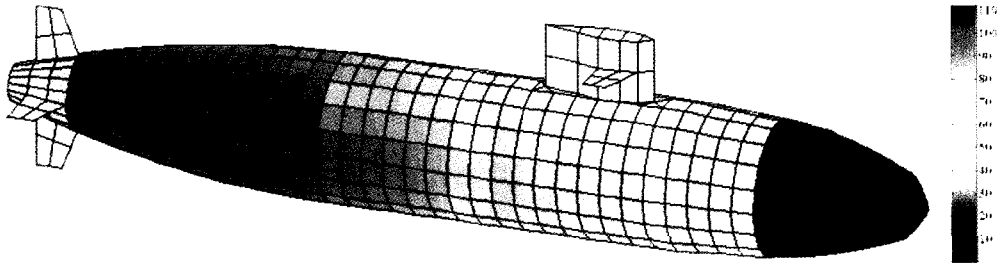

(a) Exterior

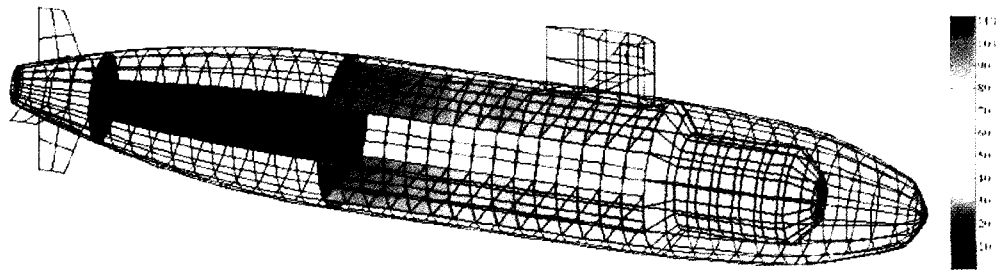

(b) Interior

Figure 4: Flexural energy density fields when f=2kHz and η=0.01

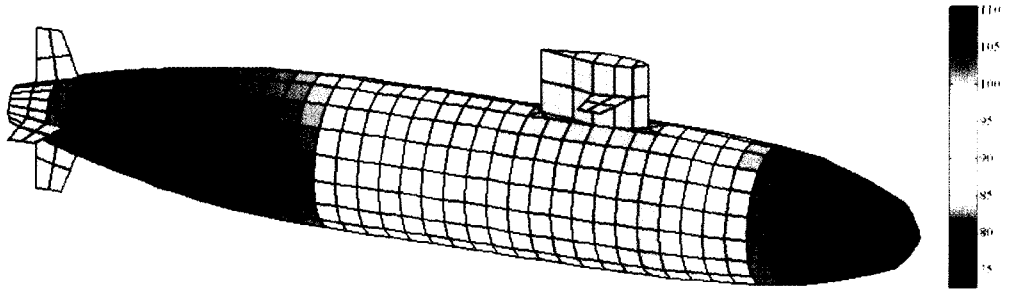

(a) Exterior

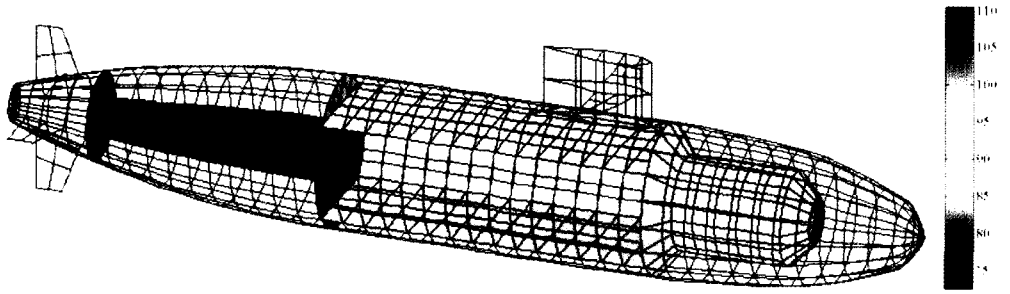

(b) Interior

Figure 5: Flexural energy density fields when f=200kHz and η=0.01

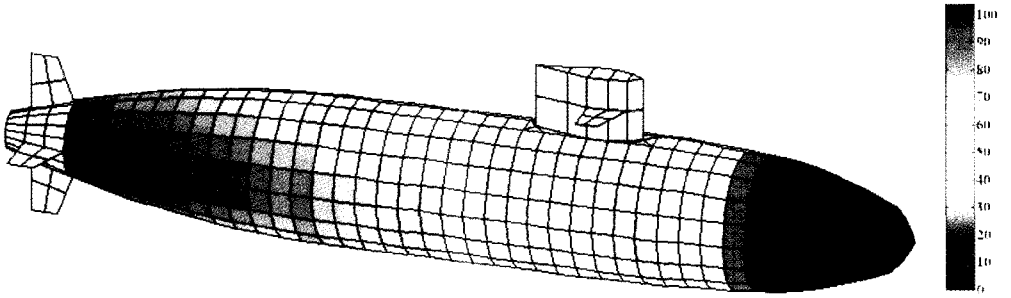

(a) Exterior

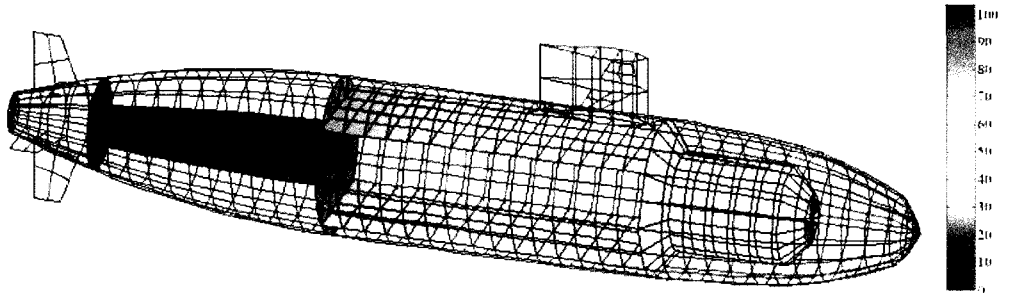

(b) Interior

Figure 6: Flexural energy density fields when f=2kHz and η=0.05(engine room parts), η=0.01(the other parts)